A Platinum Open Access Journal for Organic Chemistry

Paper

Free to Authors and Readers | DOAJ Seal | *Arkivoc* **2024** (1) 202412224

A DFT study of mono-, bi- and tricyclic examples of semi-conjugated heterocyclic mesomeric betaines

Wojciech P. Oziminski*[a] and Christopher A. Ramsden*[b]

[a]*Department of Organic and Physical Chemistry, Faculty of Pharmacy, Medical University of Warsaw, 1 Banacha Street,02-097 Warsaw, Poland*

[b]*Lennard-Jones School of Chemical and Physical Sciences Keele University, Staffordshire ST5 5BG, UK*

Email: wojciech.oziminski@wum.edu.pl, c.a.ramsden@keele.ac.uk

Dedicated to the memory of Alan Katritzky and Charles Rees

Received 05-20-2024 **Accepted** 06-06-2024 **Published on line** 06-12-2024

Abstract

The properties of heterocyclic mesomeric betaines (HMBs) are determined by the connectivity between the ring 2π heteroatoms and the odd conjugated fragments that complete the ring. In contrast to conjugated HMBs (1,3-dipoles) and cross-conjugated HMBs (1,4-dipoles), semi-conjugated HMBs are a class of heterocycle that is unexplored. The only known example is 1,4-dimethyl-1,2,4,5-tetrazinium-3,6-diolate. In this study density functional theory (DFT) methodology is employed to further investigate the structures and properties of examples of mono- bi- and tricyclic semi-conjugated HMBs. A common feature associated with the 'semi-conjugation' is a small energy gap between the frontier orbitals.

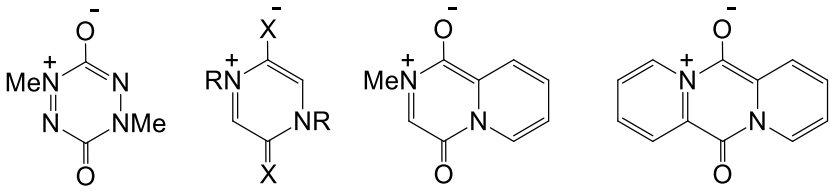

Keywords: Betaine, semi-conjugated, 1,4-diazinium-3,6-diolate, aromaticity, antiaromaticity, density functional theory (DFT), frontier orbitals

Cite as *Arkivoc* **2024** (1) 202412224
DOI: https://doi.org/10.24820/ark.5550190.p012.224

Introduction

Heterocyclic chemistry is a relatively mature science; Runge detected pyrrole in 1834 and Anderson isolated pyridine in 1846. Nevertheless, there are still many heterocyclic rings that remain unknown and, more surprisingly, some for which only a single, stable, crystalline example has been fully characterised but no further work on derivatives or analogues has been reported. One example is the 3,6-dioxo-1,2,4,5-tetrazinium derivative **1** which was prepared as dark blue plates (mp 146 °C) by Neugebauer and co-workers in 1984.[1] Both the structure and the properties of this mesomeric betaine are of some interest. Using connectivity-matrix analysis,[2] three main types of heterocyclic mesomeric betaine (HMB) have been recognised:[3,4] (i) conjugated HMBs which are associated with 1,3-dipoles, e.g., **2**;[5] (ii) cross-conjugated HMBs which are associated with 1,4-dipoles, e.g., **3**;[6] and (iii) semi-conjugated HMBs which are a smaller class whose properties are unexplored. Structure **1** is currently a unique example of a fully characterised semi-conjugated HMB.

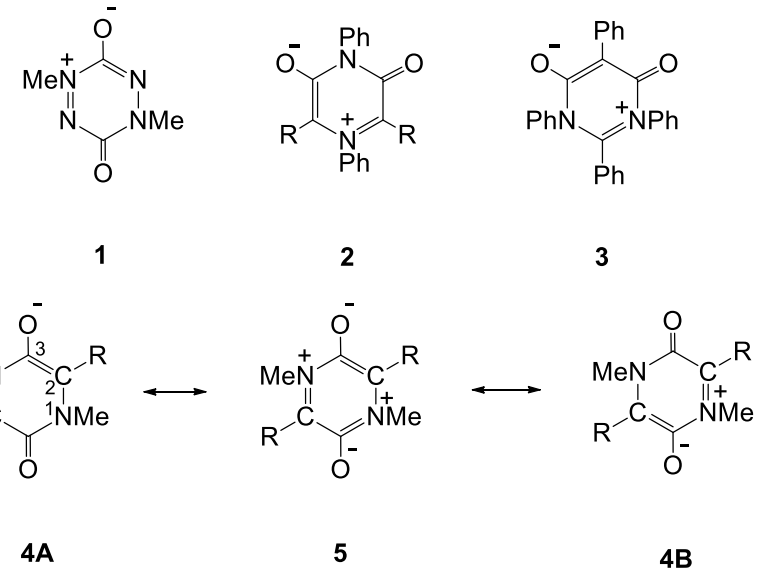

The simplest examples of monocyclic semi-conjugated mesomeric betaines are the 1,4-diazinium derivatives **4**. An unusual feature of semi-conjugated betaine rings is that equivalent dipolar resonance forms, e.g., **4A** and **4B**, can only be interconverted via an intermediate tetrapolar resonance structure, e.g., **5**. In an earlier study, using density functional theory (DFT) methods, we investigated the properties of a range of 2,5-disubstituted derivatives **4** and identified significant quantitative relationships between ring structure and the properties of the substituents R.[7] In particular, π-electron-donating substituents favour planar structures with higher aromaticity indices [HOMA, $NICS(1)_{zz}$] and π-electron-withdrawing groups favour non-planar chair or boat structures with increased antiaromatic character. A common calculated feature of the derivatives **1** and **4** is a small energy gap between the frontier orbitals, which is characteristic of antiaromaticity, and may be a desirable property for some applications.

Semi-conjugated HMBs show features of both aromatic and antiaromatic character. To further explore the properties of this little known class of heterocyclic molecules, we now report a study of the effect of N-substituents on the properties of the 1,4-disubstituted rings **6** (Table 1) together with a study of bicyclic analogues **7** (Table 2) and tricyclic derivatives **8** – **13** (Tables 3 and 4).

Results and Discussion

1. Monocyclic derivatives. Table 1 shows the effect of selected substituents at the 1,4 and 3,6 positions of the 1,4-diazonium derivatives **6**. Replacement of methyl substituents **6b** by protons **6a** or phenyl substituents **6c** has little effect on the ring geometry. The phenyl substituents are twisted from the plane of the heterocyclic ring by 51.3°. There are small variations in the frontier orbital energies but the frontier orbital gaps do not significantly vary (2.4 ± 1.5 eV); there is a small decrease in aromatic character [HOMA, $NICS(1)_{zz}$] when N-Me is replaced by either N-H or N-Ph but this is not significant. The index pEDA (pi Electron Donor Acceptor) is a measure of the π population and is the sum of the $2p_z$ atomic orbital population minus the aromatic sextet value of six.[8,9] The values in Table 1 vary between 0.7 and 0.9 which is consistent with a 7π system as represented by structures **6**.

Table 1. DFT Calculated Energies, Geometries and Aromaticity Indices of HMBs **6**

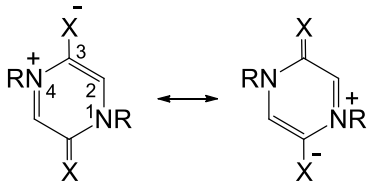

6A **6B**

				Bond Length (Å)				Bond Angle (°)
Structure	R	X	G[a]	N1-C2	C2-C3	C3-N4	C3-X	C2-C3-N4
6a	H	O	-414.824048	1.345	1.424	1.416	1.231	110.8
6b	Me	O	-493.417313	1.346	1.418	1.420	1.236	112.5
6c	Ph	O	-876.876152	1.352	1.418	1.433	1.232	112.2
6d	CHO	O	-641.514067	1.350	1.419	1.447	1.227	112.0
6e	Me	S	-1139.352549	1.342	1.403	1.408	1.692	113.2
6f	Me	NCN	-638.139786	1.341	1.409	1.395	1.324	114.8
Structure	R	X	HOMO[b]	LUMO[b]	FMOgap	pEDA	HOMA	$NICS(1)_{zz}$
6a	H	O	-5.677	-3.283	2.39	0.81	0.678	-8.6751
6b	Me	O	-5.351	-2.813	2.54	0.81	0.684	-10.3882
6c	Ph	O	-5.280	-3.038	2.24	0.82	0.602	-7.0098
6d	CHO	O	-6.325	-4.653	1.67	0.70	0.512	-4.9174
6e	Me	S	-5.317	-3.261	2.06	0.86	0.809	-4.1698
6f	Me	NCN	-6.036	-4.012	2.02	0.82	0.844	-6.8021

[a]Hartrees, [b]electron volts (eV)

N-Formyl substituents **6d** result in some shortening of the exocyclic C-O bonds and lengthening of the C3-N4 and C6-N1 bonds, presumably due to some conjugation with the formyl groups, which are planar with the ring. The π-electron withdrawing character of this substituent (CHO) is reflected by the low value of the pEDA index for **6d**. These substituents lower the energies of the frontier orbitals, significantly reduce the FMO gap (1.67 eV) and reduce the aromatic character relative to **6a** – **6c**. The use of NICS values to measure magnetic aromaticity without further evidence of current density has been criticised.[10,11] We have therefore used the

anisotropy of induced current density (ACID) method[12] to investigate electron delocalisation in rings **6b** and **6d**. The observed π + σ and π electron current maps are shown in Figure 1. Close inspection reveals that there is much less cyclic conjugation in **6d** relative to that in **6b**, which is consistent with the observed NICS(1)$_{zz}$ values (Table 1). The ACID maps support higher aromaticity of **6b** versus **6d** as there is much more visible ring current in **6b**. Overall, the results suggest that formamide derivatives **6d** and other amide derivatives can be expected to have higher reactivity (low LUMO) and less thermodynamic stability [HOMA, NICS(1)$_{zz}$] than N-methyl derivatives. Based on the results for derivatives **6a**-**d**, N-alkyl and N-aryl substituents appear to have optimal properties for the rings **6** and investigation of other, less practical, N-substituents was not undertaken.

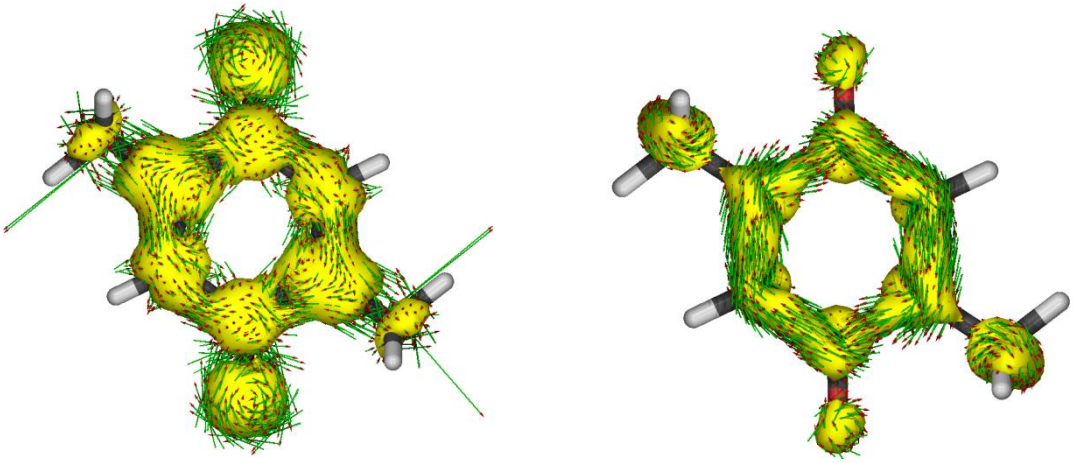

(i) **6b** (R = Me, X = O) **(ii)**

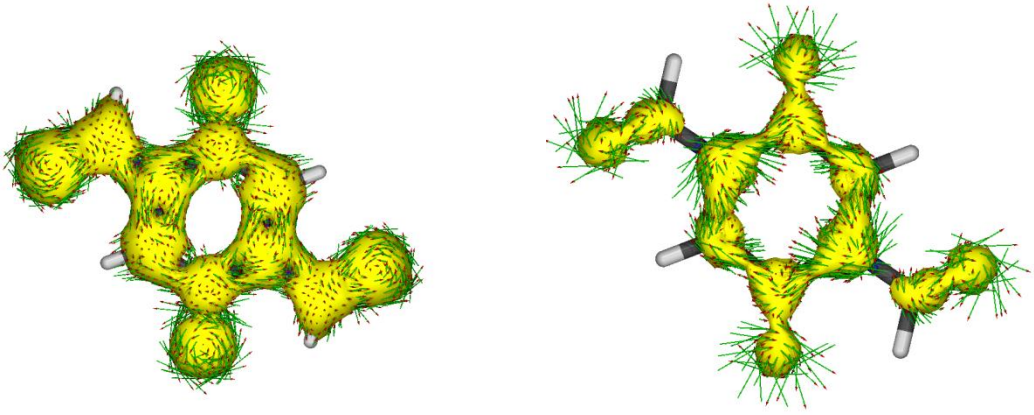

(i) **6d** (R = CHO, X = O) **(ii)**

Figure 1. ACID π + σ (i) and π (ii) electron current density maps for structures **6b** and **6d**.

We have previously investigated the 3,6-dithio derivative **6e**. Replacement of exocyclic C=O by C=N-CN (**6f**) results in shortening of all the ring bonds relative to the dioxo analogues **6a**-**d** (Table 1). As in derivative **6d**, the extended conjugation lowers the frontier orbital energies and results in a smaller FMO gap (2.02 eV) comparable to that of the dithio analogue **6e** (2.06) (Table 1). The classical aromaticity (HOMA) appears to increase relative to the dioxo analogues, probably due to the bond shortening, but the magnetic aromaticity [NICS(1)$_{zz}$] is lower than that of the derivative **6b**. In fact the calculated properties of the C=N-CN derivative **6f** are not dissimilar to those of the known derivative **1** [HOMO: -6.48; LUMO: -4.16; FMOgap: 2.32 eV; pEDA: 0.91; HOMA: 0.70; NICS(1)zz: -7.2] and C=N-CN may be a suitable functional group for stabilising the semi-conjugated ring. We next turned our attention to bicyclic and tricyclic derivatives.

2. Bicyclic derivatives. The results for calculations on four bicyclic derivatives are shown in Table 2. These are the parent structure **7a** and three aza derivatives **7b**-**d**. In all four examples, relative to the monocyclic structure **6b**, the presence of the second ring results in lengthening of the N1-C2 and C2-C3 bonds, shortening of the C3-N4 bonds and little effect on the C-O bond lengths of the 1,4-diazonium ring. For the parent structure **7a**, both the HOMO and LUMO energies are slightly higher in energy than for the monocyclic ring **6b** but the FMO gap is similar (2.42 vs 2.54 eV) (Table 2). Figure 3 shows the distribution of HOMO and LUMO for structure **7a**. As expected, due to the electronegativity of nitrogen, the frontier orbital energies of derivatives **7b** and **7c** are lower but the FMO gap is similar to **7a**. Even for the 5-aza derivative **7d**, for which the effect on HOMO energy is greatest, the FMO gap is only just outside the range 2.4 ± 1.5 eV.

Table 2. DFT Calculated Energies, Geometries and Aromaticity Indices of HMBs **7**

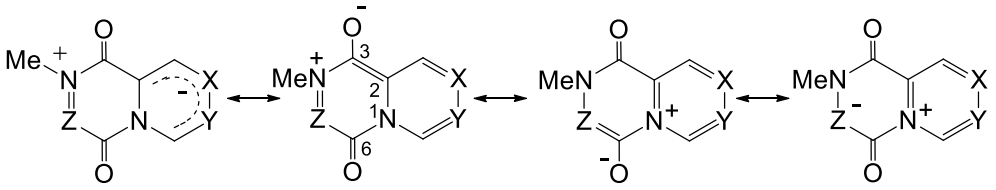

					Bond Length (Å)				
Structure	X	Y	Z	G[a]	N1-C2	C2-C3	C3-N4	C3-O	C6-O
7a	CH	CH	CH	-607.754562	1.380	1.460	1.380	1.236	1.236
7b	N	CH	CH	-623.799817	1.381	1.452	1.394	1.231	1.234
7c	CH	N	CH	-623.803630	1.381	1.454	1.386	1.234	1.233
7d	CH	CH	N	-623.796199	1.356	1.476	1.362	1.234	1.220
Structure	X	Y	Z	HOMO[b]	LUMO[b]	FMOgap	pEDA	HOMA	$NICS(1)_{zz}$
7a	CH	CH	CH	-5.081	-2.667	2.41	0.94	0.385	-10.967
7b	N	CH	CH	-5.502	-3.206	2.30	0.88	0.494	-13.204
7c	CH	N	CH	-5.394	-3.083	2.31	0.90	0.436	-12.904
7d	CH	CH	N	-5.740	-3.115	2.62	1.05	-0.127	-3.757

[a] Hartrees, [b] electron volts (eV)

The π-electron density in the betaine ring of the bicycles **7**, measured by pEDA, is increased relative to the monocycles (Table 1). For the derivatives **7a-c** this can be attributed to an increased contribution of the resonance forms **7A** in which conjugation into the second ring draws in electron density from the ring substituents. This effect can be expected to be associated with lower aromaticity. This is certainly reflected in the HOMA indices of classical aromaticity for **7a**-**c** (Table 2). However, for these derivatives the magnetic aromaticity index [$NICS(1)_{zz}$] remains comparable to that of **6b**.

For derivative **7d** the pEDA value is particularly high (1.05) and the magnetic and classical aromaticity are much lower, suggestive of some antiaromatic character. This may be attributed to the electronegative nitrogen atom at position 5 leading to a greater contribution of resonance forms of the type **7D**.

3. Tricyclic derivatives. Calculated results for the tricyclic derivative **8a** and two diaza analogues are shown in Table 3. The rings are planar. It is notable that for these derivatives the N1-C2 and N4-C5 bonds are significantly

longer than in the mono- and bicyclic analogues **6** and **7** whereas the other ring bonds are close to the monocyclic values. The frontier orbital energy levels for **8a** are not dissimilar to those of **6b** and **7a** and the FMO gap (2.20 eV) is slightly smaller. In agreement with the frontier orbital maps (Figure 3), aza substitution significantly lowers the HOMO and LUMO energies and **8b** has lower frontier orbital energies than **8c**.

The pEDA values for the derivatives **8a-c** are of some interest. For the parent structure **8a** the value is 0.97 is high but consistent with the resonating structures **8B** ↔ **8C** (Table 3). For the aza derivatives **8b,c** the pEDA value is halved together with some shortening of the C=O bonds. This implies polarisation of π-electrons away from the central ring and can be rationalised in terms of increased contributions from the resonance hybrids **8A** and **8D** (Table 3).

Table 3. DFT Calculated Energies, Geometries and Aromaticity Indices of HMBs **8**

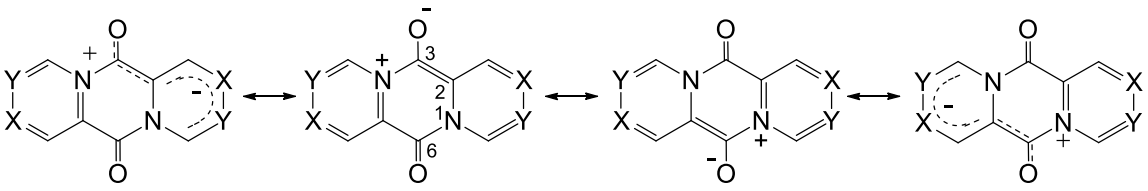

8A **8B** **8C** **8D**

				Bond Length				
Structure	X	Y	G[a]	N1-C2	C2-C3	C3-N4	C3-O	C6-O
8a	CH	CH	-722.081556	1.400	1.432	1.421	1.235	1.235
8b	N	CH	-754.176895	1.393	1.435	1.422	1.229	1.229
8c	CH	N	-754.183300	1.398	1.432	1.425	1.231	1.231
Structure	X	Y	HOMO[b]	LUMO[b]	FMOgap	pEDA	HOMA	$NICS(1)_{zz}$
8a	CH	CH	-4.809	-2.605	2.20	0.97	0.462	-18.999
8b	N	CH	-5.600	-3.535	2.07	0.50	0.458	-17.482
8c	CH	N	-5.397	-3.291	2.11	0.48	0.446	-17.884

[a] Hartrees, [b] electron volts (eV)

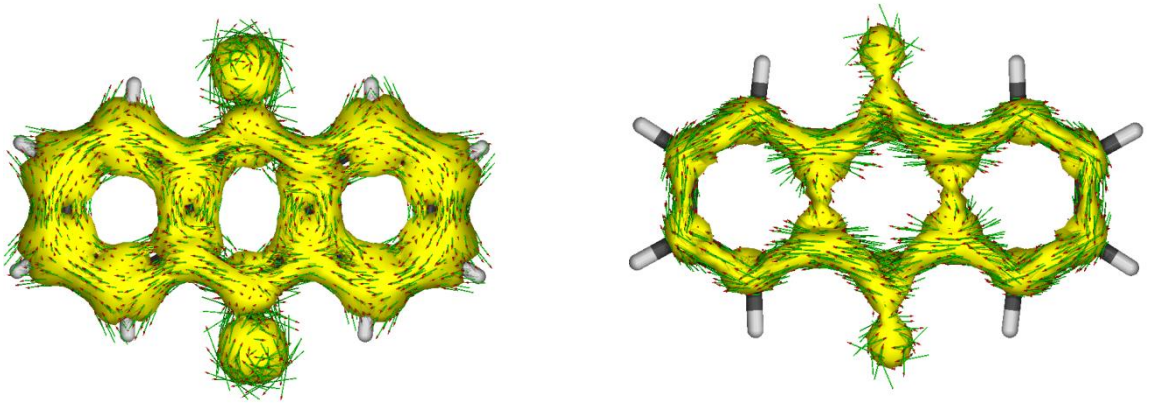

(i) **(ii)**

Figure 2. ACID π + σ (i) and π (ii) electron current density maps for structure **8a**.

Aza substitution has little effect on the aromaticity indices. The HOMA values are low (0.45-0.46) compared with the monocycle **6b** (0.68) indicating decreased classical aromaticity. The NICS(1)$_{zz}$ values, in contrast, are quite high (-17.5 to -19.0) (benzene -29.76) which is greater than for mono- and bicyclic derivatives (Table 1 and 2) and indicative of a significant ring current, attributable to enhancement by the 14-atom periphery. The ACID plots for structure **8a** are shown in Figure 2. Both the π + σ and π-only ACID plots confirm the high aromaticity expressed by the NICS(1)$_{ZZ}$ value of -19. It is worth noticing that the ring current goes over the envelope of all three rings which is especially well seen in the π-only plot.

For structure **8a** the peripheral rings have the following parameters: HOMA = 0.78, pEDA = 0.47. Thus the π-excess of these peripheral rings is much smaller and HOMA aromaticity higher showing high aromaticity for the whole molecule.

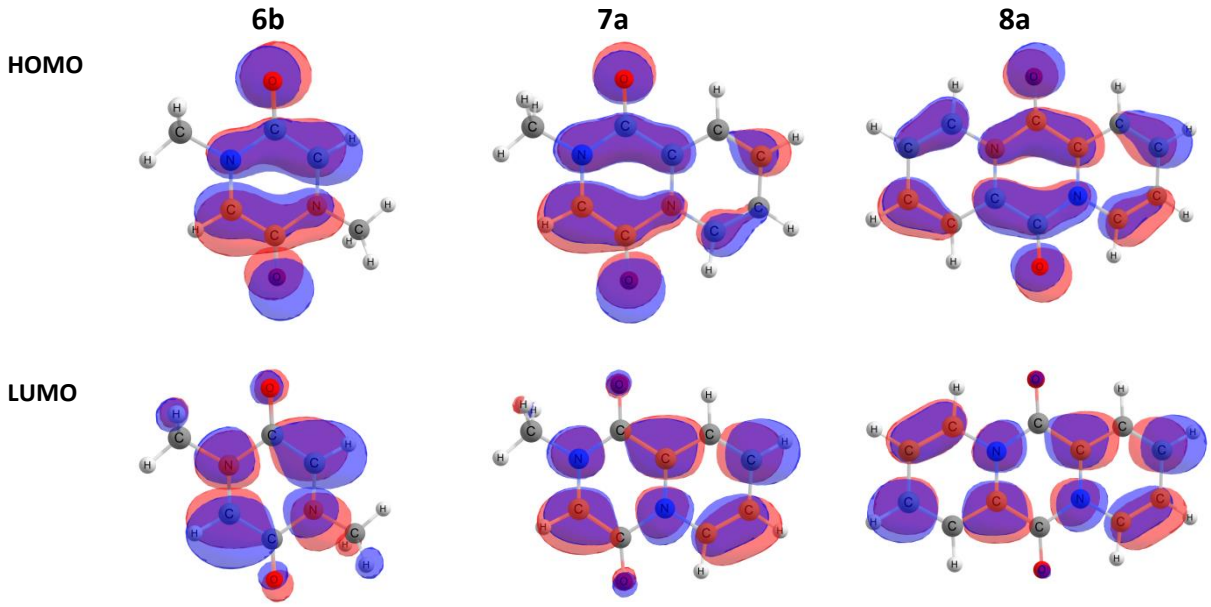

Figure 3. Calculated frontier orbitals for structures **6b**, **7a** and **8a**.

Although only one example of a semi-conjugated mesomeric betaine is known (i.e., **1**), the number of possible polycyclic example is quite large. To explore the general properties of this class further, we have calculated properties of the five tricyclic molecules **9**- **13** and the results are shown in Table 4. Like structure **8a**, structures **9** and **10** have an element of symmetry. Structure **9** is calculated to be planar but structures **10** and **11** are non-planar in which the central rings have a slight twist/boat conformation in which the torsion angles 2-3-4-5 are 16^{o} and 10^{o}, respectively. Based on the calculated properties it is not clear why these structures distort from planarity. They both have a phenolate fragment fused at the 2,3 position but structure **13** with a similar feature is planar. Structure **12** is also planar. A common feature of systems **8**-**13** is a pEDA value of the central ring in the range 0.8 to 1.05 and FMOgaps in the range 1.2 to 2.3 eV.

Table 4. DFT Calculated Energies, Geometries and Aromaticity Indices of HMBs **8a**, **9**-**13**

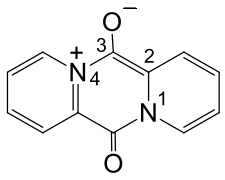

8a

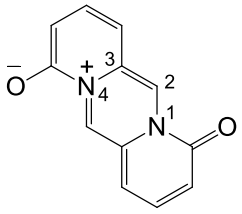

9

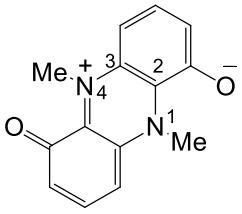

10

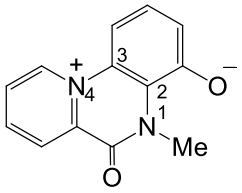

11

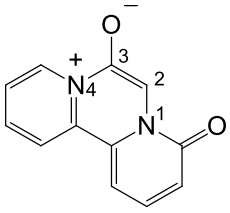

12

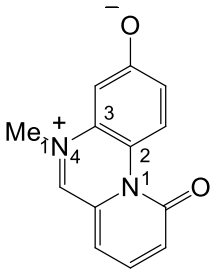

13

Structure	Bond Length N1-C2	C2-C3	C3-N4	C-O(1)	C-O(2)	HOMO[a]	LUMO[a]	FMOgap	pEDA	HOMA	NICS(1)$_{zz}$
8a	1.400	1.432	1.421	1.235	1.235	-4.809	-2.605	2.20	0.97	0.462	-18.999
9	1.410	1.381	1.346	1.223	1.223	-5.442	-3.397	2.04	0.81	0.816	-17.188
10	1.350	1.440	1.398	1.246	1.246	-5.277	-4.033	1.24	0.79	0.628	-9.477
11	1.394	1.419	1.428	1.249	1.229	-4.850	-3.344	1.51	0.90	0.420	-7.193
12	1.373	1.388	1.493	1.228	1.222	-5.252	-2.987	2.26	0.94	0.398	-10.874
13	1.401	1.449	1.410	1.242	1.222	-5.190	-3.570	1.62	1.04	0.598	-3.482

[a] electron volts (eV)

Conclusions

Semi-conjugated heterocyclic mesomeric betaines are a little known and little understood class of heterocycles and only one derivative has been characterised. The 'semi-conjugated' nature of the ring components does not facilitate rationalisation of their properties using resonance theory. The molecular orbital approach described in this study was undertaken to seek further understanding of these elusive molecules. Some common features are apparent. These molecules are associated with a small frontier orbital energy gap (FMOgap) with calculated values in the range 1.2 to 2.6 eV. In the examples studied, the HOMO energies vary in the range -6.3 to -4.8 eV and the LUMO energies in the range -4.7 to -2.6 eV.

For stability a large FMOgap is desirable with a low HOMO energy to avoid facile oxidation and a high LUMO to disfavour reduction. Inspection of Tables 1-4 reveals several candidates. For the monocycles the derivative **6f** (X = NCN) has a low HOMO (-6.04 eV) but the FMOgap (2.02) is less than desirable; nevertheless, its profile is similar to that of derivative **1**. Although the HOMOs are not as low in energy, the methyl and phenyl derivatives **6b** and **6c** have desirable properties.

For the bicyclic derivatives (Table 2) the 5-aza derivative **7d** has an interesting profile with a FMOgap of 2.62 eV and a low HOMO (-5.74 eV). The derivatives **7a-c** also have promising profiles. Among the tricycles **8a** and **12** have the most promising energy profiles.

The index pEDA varies from 0.7 to 1.05 which is indicative of the central ring approaching a 7π system as represented by structures **6**. The exceptions are derivatives **8b,c** in which both rings appear to be pulling electrons in opposite directions from the central ring.

The aromaticity indexes are not necessarily good indicators of stability, and it has been demonstrated that they do not necessarily mutually correlate;[13] they measure different molecular properties. HOMA is a geometry based aromaticity index and reflects the bond lengths in the ring and their comparison to established aromatic bond lengths. We have previously calculated the aromatic stabilisation energy (ASE) of the ring **6b** to be 18.1 kcal mol^{-1} suggesting that cyclic conjugation makes a significant contribution to stabilising the ring.[14] This corresponds to a HOMA value of 0.68 and modest aromaticity. The C=N-CN derivative **6f** has a high HOMA value (0.84), and combined with the properties mentioned above, makes it a notable derivative. The index $NICS(1)_{zz}$ is a measure of magnetic aromaticity and cyclic conjugation of electrons. With the exception of structure **7d**, the $NICS(1)_{zz}$ values for the bicyclic and tricyclic derivatives **7** and **8** are enhanced relative to monocycle **6b**. The second ring(s) appear to enhance cyclic conjugation. For reasons not clear, both aromaticity indices are particularly low for structure **7d**.

Based on aromatic stabilisation energy (ASE) and the aromaticity indices HOMA, $NICS(1)_{zz}$, semi-conjugated 1,4-diazinium-3,6-diolate rings have a modest degree of aromatic character but also a narrow HOMO-LUMO gap that is characteristic of antiaromatic species. The aromatic character can be expected to endow selected derivatives with a degree of themodynamic stability (e.g., **1**) whereas their antiaromatic characteristics makes them potentially useful for electronic applications. This combination of properties is unusual and merits closer experimental investigation.

Computational Details

All calculations were performed using the Gaussian 16 suite of programs.[15] Hybrid functional B3LYP[16,17] was used in conjunction with triple-zeta Pople basis set 6-311++G(d,p).[18,19] All geometry optimizations were followed by frequency calculations to confirm that all optimized structures are energy minima and to calculate the ZPE and thermal corrections to Gibbs free energy. Three aromaticity indices were calculated - geometric HOMA,[20,21] magnetic $NICS(1)_{ZZ}$,[22] and electronic pEDA.[8] The $NICS(1)_{ZZ}$ index was calculated as the z-component(perpendicular) of shielding constant of a ghost atom laying 1 Å above the geometric centre of the ring. ACID maps were calculated by using the software package developed by Herges and Geuenich.[23] The isovalue used for ACID calculations was the default value of 0.050.

Supplementary Material

Absolute energies and atomic coordinates of calculated structures are provided as supplementary material.

Acknowledgements

Computational Grant G36-9 from the Interdisciplinary Centre for Mathematical and Computational Modelling at Warsaw University (ICM UW) is gratefully acknowledged.

References

1. Neugebauer, F. A.; Fischer, H.; Krieger, C. *Tetrahedron Lett.* **1984**, *25*, 629-632. https://doi.org/10.1016/S0040-4039(00)99956-8
2. Ramsden, C. A. *Tetrahedron* **2013**, *69*, 4146-4159. https://doi.org/10.1016/j.tet.2013.02.081
3. Ramsden, C. A. *Prog. Heterocycl. Chem.* **2016**, *28*, 1-25. https://doi.org/10.1016/B978-0-08-100755-6.00001-6
4. Ramsden, C. A. *Adv. Heterocycl. Chem.* **2022**, *137*, 1-24.
5. Honzl, J.; Šorm, M.; Hanuš, V. *Tetrahedron* **1970**, *26*, 2305-2319. https://doi.org/10.1016/S0040-4020(01)92810-8
6. Kratky, C.; Kappe, T. *J. Heterocycl. Chem.* **1981**, *18*, 881-884. https://doi.org/10.1002/jhet.5570180506
7. Ramsden, C. A.; Oziminski, W. P. *J. Org. Chem.* **2023**, *88*, 8248-8256. https://doi.org/10.1021/acs.joc.3c00225
8. Oziminski, W. P.; Dobrowolski, J. C. *J. Phys. Org. Chem.* **2009**, *22*, 769-778. https://doi.org/10.1002/poc.1530
9. Oziminski, W. P.; Krygowski , T. M. *Chem. Phys. Lett.* **2011**, *510*, 53-56. https://doi.org/10.1016/j.cplett.2011.05.029
10. Damme, S. V.; Acke, G.; Havenith, R. W. A.; Bultinck, P. *Phys. Chem. Chem. Phys.* **2016**, *18*, 11746-11755. https://doi.org/10.1039/C5CP07170D
11. Gershoni-Poranne, R.; Stanger, A. *Aromaticity: Modern Computational Methods and Applications*, Chapter 4, ed., Fernandez, I., Elsevier, **2021**, pp 99-153. https://doi.org/10.1016/B978-0-12-822723-7.00004-2
12. Geuenich, D.; Hess, K.; Köhler, F.; Herges, R. *Chem. Rev*. **2005**, *105*, 3758-3772. https://doi.org/10.1021/cr0300901
13. Ramsden, C. A. *Tetrahedron* **2010**, *66*, 2695-2699. https://doi.org/10.1016/j.tet.2010.02.019
14. Ramsden, C. A.; Oziminski, W. P. *Tetrahedron* **2014**, *70*, 7158-7165. https://doi.org/10.1016/j.tet.2014.06.047
15. Gaussian 16, Revision B.01, Frisch, M. J.; Trucks, G. W.; Schlegel, H. B.; Scuseria, G. E.; Robb, M. A.; Cheeseman, J. R.; Scalmani, G.; Barone, V.; Petersson, G. A.; Nakatsuji, H.; Li, X.; Caricato, M.; Marenich, A. V.; Bloino, J.; Janesko, B. G.; Gomperts, R.; Mennucci, B.; Hratchian, H. P.; Ortiz, J. V.; Izmaylov, A. F.; Sonnenberg, J. L.; Williams-Young, D.; Ding, F.; Lipparini, F.; Egidi, F.; Goings, J.; Peng, B.; Petrone, A.; Henderson, T.; Ranasinghe, D.; Zakrzewski, V. G.; Gao, J.; Rega, N.; Zheng, G.; Liang, W.; Hada, M.; Ehara, M.; Toyota, K.; Fukuda, R.; Hasegawa, J.; Ishida, M.; Nakajima, T.; Honda, Y.; Kitao, O.; Nakai, H.; Vreven, T.; Throssell, K.; Montgomery Jr, J. A.; Peralta, J. E.; Ogliaro, F.; Bearpark, M. J.; Heyd, J. J.; Brothers, E. N.; Kudin, K. N.; Staroverov, V. N.; Keith, T. A.; Kobayashi, R.; Normand, J.; Raghavachari, K.; Rendell, A. P.; Burant, J.

C.; Iyengar, S. S.; Tomasi, J.; Cossi, M.; Millam, J. M.; Klene, M.; Adamo, C.; Cammi, R.; Ochterski, J. W.; Martin, R. L.; Morokuma, K.; Farkas, O.; Foresman, J. B.; Fox, D. J. Gaussian, Inc., Wallingford CT, 2016.
16. Becke, A. D. *Phys. Rev. A* **1988**, *38*, 3098-3100. https://doi.org/10.1103/PhysRevA.38.3098
17. Lee, C.; Yang, W.; Parr, R. G. *Phys. Rev. B* **1988**, *37*, 785-789. https://doi.org/10.1103/PhysRevB.37.785
18. McLean, A. D.; Chandler, G. S. *J. Chem. Phys.* **1980**, *72*, 5639–5648. https://doi.org/10.1063/1.438980
19. Clark, T.; Chandrasekhar, J.; Spitznagel, G. W.; Schleyer, P. v. R. *J. Comput. Chem.* **1983**, *4*, 294–301. https://doi.org/10.1002/jcc.540040303
20. Kruszewski, J.; Krygowski, T. M. *Tetrahedron Lett.* **1972**, *13*, 3839-3842. https://doi.org/10.1016/S0040-4039(01)94175-9
21. Krygowski, T. M. *J. Chem. Inf. Comput. Sci.* **1993**, *33*, 70-78. https://doi.org/10.1021/ci00011a011
22. Schleyer, P. v. R.; Maerker, C.; Dransfeld, A.; Jiao, H.; Hommes, N. J. R. van E. *J. Am. Chem. Soc*. **1996**, *118*, 6317-6318. https://doi.org/10.1021/ja960582d
23. Herges, R.; Geuenich, D. *J. Phys. Chem. A* **2001**, *105*, 3214−3220. https://doi.org/10.1021/jp0034426

